

SELECTIVE LASER SINTERING AND FREEZE EXTRUSION FABRICATION OF SCAFFOLDS FOR BONE REPAIR USING 13-93 BIOACTIVE GLASS: A COMPARISON

Krishna C. R. Kolan, Nikhil D. Doiphode and Ming C. Leu
Department of Mechanical and Aerospace Engineering
Missouri University of Science and Technology, Rolla, MO 65409

Abstract

13-93 glass is a third-generation bioactive material which accelerates the bone's natural ability to heal by itself through bonding with surrounding tissues. It is an important requirement for synthetic scaffolds to maintain their bioactivity and mechanical strength with a porous internal architecture comparable to that of a human bone. Additive manufacturing technologies provide a better control over design and fabrication of porous structures than conventional methods. In this paper, we discuss and compare some of the common aspects in the scaffold fabrication using two such processes, viz. selective laser sintering (SLS) and freeze extrusion fabrication (FEF). Scaffolds fabricated using each process were structurally characterized and microstructure analysis was performed to study process differences. Compressive strength higher than that of human trabecular bone was achieved using SLS process and strength almost comparable to that of human cortical bone was achieved using FEF process.

1. Introduction

The conventional treatment of a bone repair includes implanting a metallic part, generally made of stainless steel, in the defect site and fixing it with the good bone with the help of screws and plates. This could lead to infections, damage to good bone, and accumulation of metals in tissues. The disadvantages of using a metallic implant led to the usage of biopolymers, which being biocompatible were better off when compared to metallic implants. However, the biopolymers researched were passive towards new bone growth. The discovery of Bioglass by Hench L. L. led to the development of several bioactive glasses, which are based on similar compositions [1]. The main intention of research behind producing such glasses primarily was to develop a material which not only bonds with the surrounding tissue when implanted, but also actively aids in the new tissue growth. One such material, which received attention lately for its bioactivity, is 13-93 glass [2, 3].

The human body is made up of many kinds of bones varying from soft tissues to load bearing bones. A typical load bearing bone (for example: femur bone) has an outer cortical (compact) bone and inner trabecular (spongy) bone. The compressive strength of a human cortical bone ranges 130 – 200 MPa and that of trabecular bone ranges 2 – 12 MPa [4]. There are a few synthetic bone grafts, some even bioactive, which are currently available in the market, in the form of flexible strips and paste, but are limited to non-load bearing bone repairs. However, fabricating a scaffold which is bioactive, has mechanical properties comparable to a load bearing bone, and has similar geometry and internal architecture of a bone is a challenging task.

There are several traditional methods which are used to fabricate scaffolds for bone repair applications. Additive manufacturing (AM) technologies, with flexibility of fabricating complicated shapes, have an edge over the traditional methods in terms of controlling the shape, porosity and pore size. AM techniques are being widely researched in the recent times and in some cases, implantation of customized scaffolds was also demonstrated [5]. The major

limitation of AM techniques lies in directly processing the bioactive glasses to fabricate scaffolds for bone tissue engineering without using a polymeric binder during the fabrication process. The binder, if it is a biocompatible polymer, can be persevered in the scaffold which affects the mechanical properties of the scaffold. Alternatively, a non-biocompatible polymer can be used during the fabrication of scaffold, which needs to be post-processed to remove the binder and sinter the glass particles. This improves the mechanical properties of scaffold but has shrinkage associated with it.

Two AM technologies, viz. SLS and FEF, are being researched at Missouri University of Science and Technology to fabricate bioactive scaffolds for bone repair applications using 13-93 glass [6, 7]. In this paper, we make an effort to discuss some of the common aspects in both of the processes during the scaffold fabrication and how they affect the properties of the scaffold after sintering. In Section 2, the fabrication of scaffolds using the two processes is briefly described along with a brief description of the post-processing methods. The common aspects in fabrication and sintering and how they affect the pore size, porosity, microstructure and compressive strength of the scaffold are discussed in Section 3. Finally, the comparative study is concluded in Section 4.

2. Fabrication and Post-processing

2.1. Selective laser sintering (SLS)

All the SLS fabrication experiments were carried out on a commercial DTM Sinterstation 2000 machine. A detailed description of the machine and its parameters is available from literature [8, 9]. An indirect SLS method was employed in our study to establish a feasible set of SLS process parameters to fabricate scaffolds using 13-93 bioactive glass. The preparation of 13-93 glass is explained in detail in [6]. Stearic acid was used as the binder. It was mixed with 13-93 glass in two different proportions (40% and 50% binder volume) and dry ball-milled for 8 hours with ZrO₂ grinding medium. The blended powder was used as the feedstock for the SLS machine. The functional SLS parameters were identified by fabricating parts measuring (25.4 x 25.4 x 1) mm and by visual inspection. Once established, a CAD model with a designed porosity and pore size was used to fabricate a cylindrical scaffold. The details regarding the fabrication and effects of parameters are available from [6].

2.2. Freeze extrusion fabrication (FEF)

The fabrication of 13-93 parts was also done using an FEF system setup, which was developed at Missouri University of Science and Technology. The entire setup is encased in a freezer box, which can be used to produce freezing temperatures down to -30°C by means of liquid nitrogen. The paste holder is enclosed in a heating sleeve with an Omega DP7002 temperature controller to prevent the paste from freezing in the syringe. A detailed description of the FEF setup and fabrication of parts is available from [10, 11, 7]. 3D scaffold fabrication was carried out by using a paste prepared by mixing 3.9 gm Aquazol[®] 50, 0.5 gm EasySpere dispersant, 0.5 gm Surfrol surfactant, 1 gm of PEG-400 lubricant and 1 gm of Glycerol with 100 gm of bioactive 13-93 glass powder in deionized water.

2.3. Post-processing

All the powders and binders used for fabrication of 13-93 scaffolds were examined by differential scanning calorimetry (DSC) (TA Instruments, SDT Q600, Utah) and differential

thermal analysis (DTA) (NETZSCH simultaneous DTA/TGA). The heat treatment schedules for the scaffolds fabricated using SLS and FEF were based on the DSC and DTA/TGA graphs. The key temperatures, viz. melting and decomposition temperatures of the binder, were obtained from the graphs. The rate of heating and the hold times were decided based on the graphs. All the green parts were post-processed in a three-stage programmable air furnace (Vulcan Benchtop Furnace, York, PA). SEM (Hitachi S-4700 FESEM, Japan) images of fracture surfaces of green parts and sintered parts were obtained to study the effect of heat treatment schedule. Mechanical testing was performed on the sintered scaffolds to determine their compressive strength using a mechanical loadframe (Instron 4469 UTM, Norwood, MA). All the tests were carried out at a cross-head speed of 0.5 mm/min.

3. Comparison and Discussion

A comparison of the two AM processes is briefly discussed in this section. The common aspects which are important and occur in both of the processes are considered. Section 3.1 gives a brief overview of the important aspects during the fabrication and post-processing stages. The limitations and advantages of the pore size and porosity of the scaffolds fabricated by each of the two processes are discussed in Section 3.2. Possible reasons between the differences in compressive strengths of the scaffolds fabricated by the two processes are analyzed in Section 3.3. Finally, SEM images of the green parts and sintered parts are shown in Section 3.4, and they are used to analyze the reasons for formation of voids.

3.1. Fabrication and post-processing

The basic differences in fabrication lie in the type of feedstock used in the two processes. SLS is a powder based technique and FEF is an aqueous paste based technique. In the SLS process, either the actual part material (13-93 glass) or the blended powder of actual part material mixed with a binder (generally a polymer) is used as feedstock for the machine. In the FEF process, 13-93 glass powder, binder, surfactant and dispersant are mixed in different quantities with de-ionized water to form a semi-solid paste with a specific viscosity to achieve a uniform extrusion through a nozzle. In the SLS process, a smaller particle size ($\sim 2 \mu\text{m}$) led to warping issues [12]. Also, smaller particles compared to larger particles will have a greater surface area, which would require higher amounts of binder to fuse the particles in the layer and to fuse the current layer with the previous layer. Hence, 13-93 glass particles used for the SLS study were sieved with a $75 \mu\text{m}$ mesh in our study. In the FEF process, 13-93 glass with a mean particle size of $2 \mu\text{m}$ was used. The importance of smaller particle size and particle size distribution in achieving better green densities and sintering results has been previously studied [13, 14]. The fusing of successive layers in indirect SLS depends on the amount of binder melted and percolated into the previous layer, whereas in FEF it is achieved by joining of the extruded paste with the previous layer by means of adhesive forces and mixing of paste at the areas of contact. The joining of two layers in FEF can be seen in the SEM image shown in Figure 1. The analysis of SEM images (in Section 3.4) of the fabricated green parts shows higher green densities and better consolidation between 13-93 glass particles in the FEF process because of 7 wt. % binder (including surfactant and dispersant) used when compared to 20 wt. % binder used in the SLS process. A longer heat treatment schedule would be required for FEF green parts, as there is surfactant and dispersant besides the binder used in the paste, when compared to only binder used in the SLS process. The average shrinkage of the sintered parts when compared to green parts fabricated using FEF was measured to be around 23% in length and width. The average

shrinkage in SLS was measured to be around 23% in length and 18% in diameter. Even with less binder used in FEF, shrinkage in the fabricated parts after sintering is similar to that of SLS because of densification of fine glass particles.

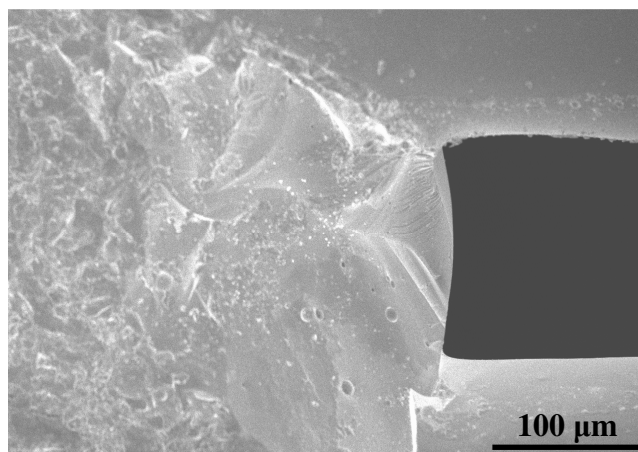


Figure 1. SEM image of FEF scaffold shows the joining of two layers.

3.2. Pore size and porosity

A wide variation in controlled pore sizes can be achieved using FEF process, which mainly depends on the size of the nozzle used during the extrusion process. Scaffolds varying in the pore size (as low as 50 μm and as high as 1 mm) can be fabricated with an appropriate selection of parameters including particle size, nozzle diameter and paste composition. In our current study, the porosity achieved for FEF scaffolds when sintered at 700°C for 1 hr was around 50% and the pore sizes varied from 500 μm to 900 μm . One of the major limitations of SLS process lies in fabricating a scaffold (green part) with pore size less than its laser spot diameter [15]. Advances in SLS machines might solve this problem in future. Even if a scaffold is fabricated with smaller pore size, removing the unsintered powder particles from small pores could be difficult. If an indirect SLS process with a sacrificial binder is used, the pore size required for bone growth can be achieved in the sintered part as the binder burns out and the green part shrinks uniformly, which leads to reduced pore widths. In our current study, the pore size achieved in a green part varied from 800 μm to 1 mm. After post-processing the green part, the pore width in the sintered scaffold varied from 300 μm to 800 μm , which makes it suitable for bone tissue growth [16]. The apparent porosities of the scaffolds fabricated using SLS varied from 50% to 60%, when sintered at different soaking conditions from 675°C to 700°C. Figures 2 and 3 show the optical images of the sintered scaffolds fabricated using FEF and SLS processes.

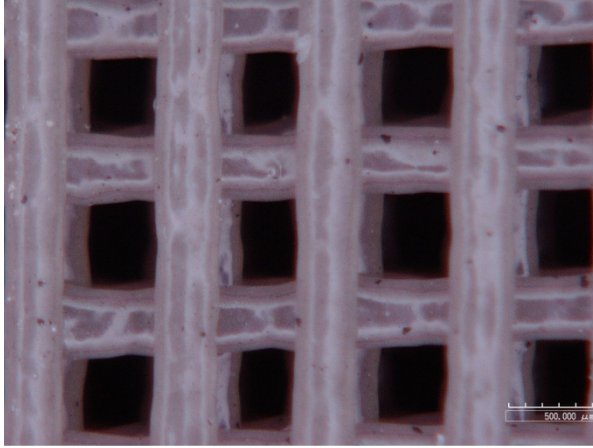


Figure 2. Sintered FEF scaffold.

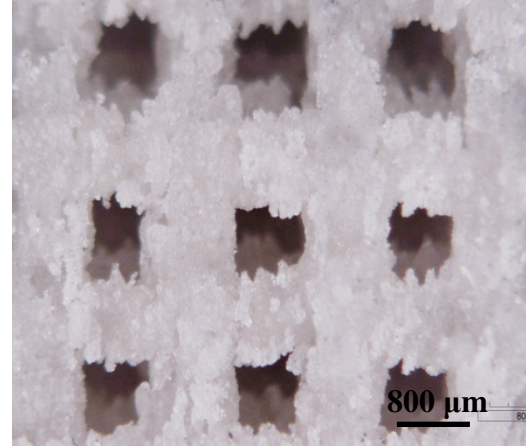


Figure 3. Sintered SLS scaffold.

3.3. Compressive strength

FEF scaffolds measuring (5 x 5 x 5) mm and SLS scaffolds measuring 16 mm in length and 8 mm in diameter were used in the compression tests on an Instron machine, as mentioned earlier. The average compressive strength of FEF scaffolds sintered at 700°C for 1 hr was measured 136 ± 73 MPa and that of SLS scaffolds sintered at 695°C for 1 hr was measured 20.4 ± 2.2 MPa. The main reasons for the difference between the mechanical strengths of the fabricated scaffolds using the two processes are particle size, process difference and the amount of binder used. A smaller particle size ($\sim 2 \mu\text{m}$) used in the FEF process together with the lower amount of binder gives good green densities and facilitates good sintering between the particles, which provides a higher compressive strength for the scaffolds. In contrast, a wider particle size distribution ($< 75 \mu\text{m}$) in the SLS process combined with a relatively high amount of binder creates voids in the course of binder burnout and sintering, which is a main reason for a relatively low strength of SLS scaffolds when compared to FEF scaffolds. Moreover, the voids are formed in the green part because of the lower green densities (SEM images shown in section 3.4), which remain and sometimes even grow in size after binder burnout and sintering. To avoid voids after the sintering and achieve near theoretical density, a smaller particle size with a narrow particle size distribution is preferred than having a larger particle size with a wider particle size distribution [13]. The voids formed in indirect SLS can be reduced with a proper combination of particle size and binder content, both of which are not considered in the current study but will be investigated in the future.

In our current study, compressive strengths measured for the scaffolds fabricated using FEF are comparable to human cortical bone. This provides the advantage of fabricating load bearing scaffolds using FEF, which can be used for both cortical and trabecular bone repair applications, by varying the porosity and pore size of scaffolds for specific applications. However, designing a complex shape (for example, femur head) could be difficult using FEF, unlike SLS, which can be used to fabricate complex parts with ease. In our current study, the compressive strength of the scaffolds fabricated using SLS is higher than that of the human trabecular bone. As discussed above, with optimized particle size and binder content using indirect SLS, the mechanical properties of the SLS scaffolds can be further improved for load bearing applications.

3.4. Microstructures

SEM images of the fractured surfaces of the scaffolds fabricated using both processes before and after sintering were analyzed. Figure 5 shows the SEM images of fractured surfaces of representative green parts fabricated by FEF and SLS. Compact packing of fine 13-93 glass particles can be seen in Figure 5(a), which is taken at a magnification of 600x. In contrast, 13-93 glass particles varying in size in a stearic acid matrix can be seen in Figure 5(b). The voids present in the SLS green part can also be observed, which become even larger after the binder burnout stage because of the higher amount of binder used in the fabrication process. Figure 6(a) shows the SEM image of the fractured surface of an FEF scaffold sintered at 700°C for 1 hr. Negligible voids and micro pores ($< 10 \mu\text{m}$) are marked in the image. Figure 6(b) shows the SEM image of the fractured surface of a SLS scaffold sintered at 685°C for 1 hr with voids measuring $\sim 300 \mu\text{m}$. Alongside the voids, the residual pores ($\sim 20 \mu\text{m}$) in the SEM image are formed because of the wider particle size distribution used in the SLS process. The importance of micro pores in the scaffold walls and rough surface in tissue engineering was previously studied [17]. The rough surface of SLS scaffolds can be seen in Figure 3 and the smooth surface of FEF scaffolds can be seen in Figure 2. The SLS scaffolds have micro pores and a rough surface, which could assist in better cell adhesion, growth and differentiation, when compared to the smooth surface of FEF scaffolds during the cell culture.

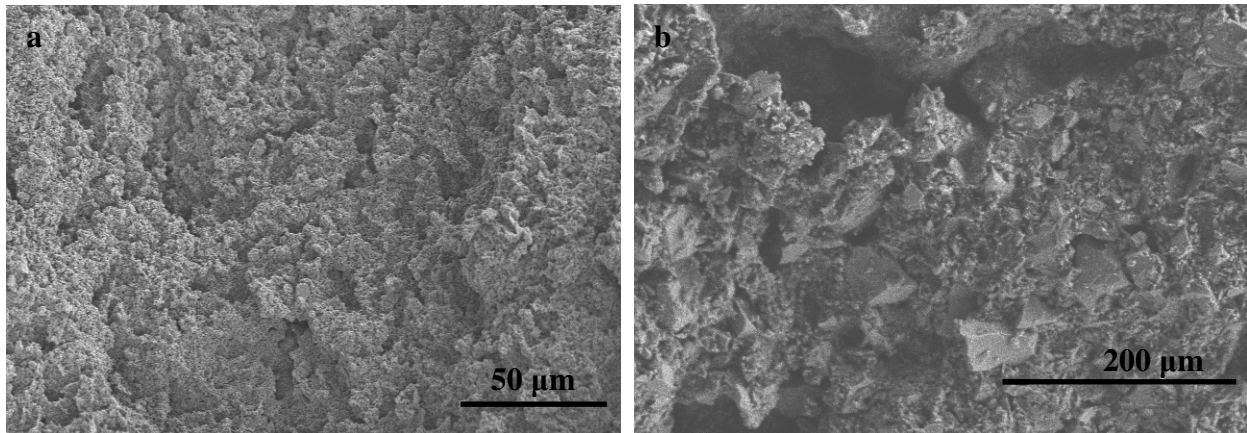


Figure 5. Fracture surfaces of green parts (a) FEF (b) SLS.

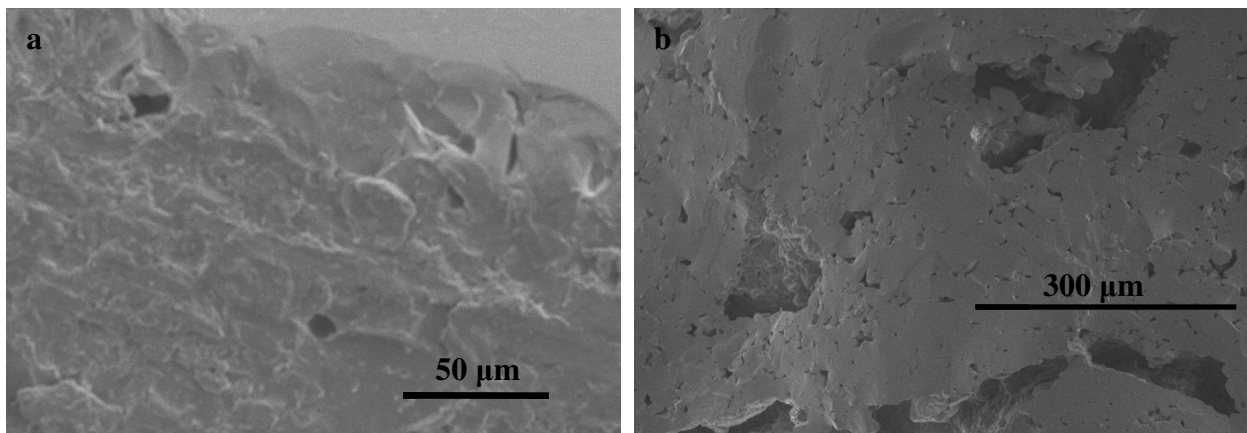


Figure 6. Fracture surfaces of sintered scaffolds (a) FEF (b) SLS.

4. Conclusions

The lower amount of binder and smaller particle size used in the FEF process when compared to the higher amount of binder and larger particle size used in the SLS process gave the FEF scaffold a higher green density in the green part, resulting higher compressive strength in the sintered part. However, a smaller particle size with optimized binder content could improve the mechanical properties of the SLS scaffolds in future studies for load bearing applications. The rough surface on the SLS scaffolds could have an advantage in cell adhesion and differentiation during cell culture when compared to the smooth surface of the FEF scaffolds. The SEM images of the fractured surfaces of the scaffolds were analyzed to study the voids and residual pores responsible for the mechanical properties.

Acknowledgement

The research work was funded by National Science Foundation under NSF SBIR phase I award #0912019 to Mo-Sci Corporation, as well as by the Intelligent Systems Center and the Center for Bone and Tissue Repair and Regeneration at Missouri University of Science and Technology.

References

- [1] M. N. Rahaman, R. F. Brown, B. S. Bal, and D. E. Day, "Bioactive Glasses for Nonbearing Applications in Total Joint Replacement," *Semin. Arthroplasty*, 17, 102–12 (2006).
- [2] R. F. Brown, D. E. Day, T. E. Day, S. Jung, M. N. Rahaman and Q. Fu, "Growth and differentiation of osteoblastic cells on 13–93 bioactive glass fibers and scaffolds," *Acta Biomaterialia*, 4, 387–396, (2008).
- [3] Q. Fu, M. N. Rahaman, W. Huang, D. E. Day and B. S. Bal, "Preparation and bioactive characteristics of a porous 13-93 glass, and its fabrication into the articulating surface of a proximal tibia," *J. Biomed. Mater. Res.*, 82A 222-9 (2007).
- [4] D. R. Carter and W.C. Hayes, "Bone compressive strength: the influence of density and strain rate," *Science*, 194, 1174–1176 (1976).
- [5] J. Cesarano III, J. G. Dellinger, M. P. Saavedra, and D.D. Gill, "Customization of Load-Bearing Hydroxyapatite Lattice Scaffolds," *Int. J. Appl. Ceram. Technol.*, 2 [3] 212–220 (2005).
- [6] K. C. R. Kolan, M. C. Leu, G. E. Hilmas and M. Velez, "Selective Laser Sintering of 13-93 Bioactive glass," *Proceedings of Solid Freeform Fabrication Symposium*, Austin, Texas, August 9-11, (2010).
- [7] N. D. Doiphode, "Freeze Extrusion Fabrication of 13-93 Bioactive glass scaffolds for bone repair," Thesis (MS), Missouri University of Science and Technology, Rolla, Missouri (2010).
- [8] M. C. Leu, E. B. Adamek, T. Huang, G. E. Hilmas and F. Dogan, "Freeform Fabrication of Zirconium diboride parts using Selective Laser Sintering," *Proceedings of Solid Freeform Fabrication Symposium*, Austin, Texas (2008).
- [9] M. C. Leu, S. Pattnaik and G. E. Hilmas "Optimization of Selective Laser Sintering process for fabrication of Zirconium diboride parts Using," *Proceedings of Solid Freeform Fabrication Symposium*, Austin, Texas (2010).
- [10] T. S. Huang, M. Mason, G. E. Hilmas and M. C. Leu, "Freeze-form Extrusion Fabrication of Ceramic Parts," *International Journal of Virtual and Physical Prototyping*, Vol. 1, No. 2, pp. 93-100 (2006).

- [11] T. Oakes, P. Kulkarni, R. G. Landers and M. C. Leu, "Development of extrusion-on-demand for ceramic Freeze-form Extrusion Fabrication," Proceedings of Solid Freeform Fabrication Symposium, Austin, Texas (2009).
- [12] S. Pattnaik, "Investigation of zirconium diboride parts using selective laser sintering," Thesis (MS), Missouri University of Science and Technology, Rolla, (2009).
- [13] J. M. Ting and R. Y. Lin, "Effect of particle-size distribution on sintering," *Journal of Materials Science*, 29 (7), pp. 1867-1872 (1994).
- [14] T. S. Yeh and M. D. Sacks, "Effect of particle size distribution on the sintering of alumina," *J. Am. Ceram. Soc.* 71 (1988), pp. C484–C487.
- [15] S. Yang, K. F. Leong, Z. Du and C. K. Chua, "The design of scaffolds for use in tissue engineering. Part II. Rapid prototyping techniques," *Tissue Eng* 8 1, pp. 1–11 (2002).
- [16] C. M. Murphy, M. G. Haugh and F. J. O'Brien, "The effect of mean pore size on cell attachment, proliferation and migration in collagen–glycosaminoglycan scaffolds for bone tissue engineering," *Biomaterials*, 31, [3], 461-466, (2010).
- [17] H. Yuan, K. Kurashina, J. D. de Bruijn, Y. Li, K. de Groot and X. Zhang, "A preliminary study on osteoinduction of two kinds of calcium phosphate ceramics," *Biomaterials* 20 (19), 1799–1806 (1999).